JACS
JOURNAL OF THE AMERICAN CHEMICAL SOCIETY
pubs.acs.org/JACS
Communication

Metal–Ligand–Anion Cooperation in C–H Bond Formation at Platinum(II)

Hannah E. Zeitler, Alexander S. Phearman, Michael R. Gau, Patrick J. Carroll, Thomas R. Cundari, and Karen I. Goldberg*

Cite This: J. Am. Chem. Soc. 2022, 144, 14446–14451
Read Online
ACCESS | Metrics & More | Article Recommendations | Supporting Information

ABSTRACT: Thermolysis of $[^{H}(BPI)Pt(CH_3)][OTf]$ (BPI = 1,3-bis(2-(4-*tert*-butyl)pyridylimino)isoindole) to release methane and form (BPI)Pt(OTf) is reported. Kinetic, mechanistic, and computational studies point to an unusual anion-assisted pathway that obviates the need for a higher oxidation state intermediate to couple the metal-bound methyl group with the ligand-bound hydrogen. Leveraging this insight, a triflimide derivative of the (BPI)Pt complex was shown to activate benzene, highlighting the role of the counteranion in controlling the activity of these complexes.

The direct functionalization of alkanes, particularly methane, is a prominent research target in catalysis.[1−3] Key in this transformation is C–H bond activation. Through studies of model transition metal systems, several distinct mechanisms have been established for this bond cleavage step that generates a metal–alkyl. Mechanisms that require a change in oxidation state, e.g., oxidative addition (OA, Chart 1a), are often contrasted with those that maintain the metal oxidation state, e.g., concerted metalation deprotonation (CMD, Chart 1b).[1,4−8] Metal–ligand cooperative (MLC, Chart 1c) mechanisms have been recently invoked.[9−12] The heterolytic H_2 activation step in Noyori's hydrogenation reactions is a classic example of MLC bond activation.[13] In C–H activation via MLC, a basic site on the ligand formally accepts the proton, with the anionic carbon fragment binding to the Lewis acidic metal. While there is no net oxidation state change at the metal, a higher oxidation state intermediate is sometimes invoked with a stepwise process of an initial OA, followed by proton transfer to the ligand.[12,14−17] Mechanisms where the oxidation state of the metal is maintained throughout the reaction are likely more robust activation paths, particularly under aerobic conditions; the electron-rich, low-valent oxidation state species required for OA can be susceptible to undesirable reactivity in preference to C–H bond activation.[1] MLC mechanisms are also attractive in terms of atom efficiency for functionalization as, in contrast to CMD, the proton remains in the coordination sphere of the metal and can potentially be incorporated into the product at a later step.

Chart 1. Mechanisms of R–H Bond Activation

a) Oxidative Addition (OA)

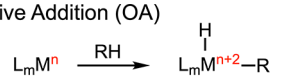

b) Concerted Metalation Deprotonation (CMD)

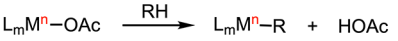

c) Metal-Ligand Cooperation (MLC)

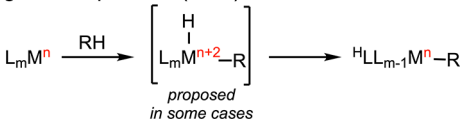

Herein we provide support for an unusual MLC mechanism for C–H coupling/activation reactions where the counteranion plays a central role in promoting the proton movement between the backbone and the carbon, and in doing so avoids a higher oxidation state intermediate. Experimental and computational mechanistic studies of the C–H coupling reaction from a $(BPI)Pt^{II}$ pincer (BPI = 1,3-bis(2-(4-*tert*-butyl)pyridylimino)isoindole) cationic methyl species are presented. Using the mechanistic understanding of this metal–ligand–anion cooperative (MLAC) reaction, a change in the counteranion allowed for benzene C–H activation. These studies of C–H coupling/activation with (BPI)Pt complexes are of particular interest, as $(BPI)Pt(CH_3)$ complexes can be aerobically functionalized.[18,19]

The reaction of triflic acid (HOTf, 1 equiv) with $(BPI)Pt(CH_3)$ (**1**) resulted in formation of $[^{H}(BPI)Pt(CH_3)][OTf]$ (**2**) (Scheme 1, 76% yield). The ^1H NMR spectrum of **2** shows broken symmetry of the BPI ligand (2 *tert*-butyl, 10 aromatic, and 1 N–H signal), consistent with protonation of one of the imine nitrogens. Obtaining X-ray-quality crystals of **2** proved challenging; however, a suitable crystal was grown of the palladium analogue, $[^{H}(BPI)Pd(CH_3)][OTf]$ (**2-Pd**, Figure 1). The solid-state structure shows asymmetry of the

Received: May 13, 2022
Published: July 26, 2022

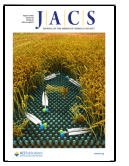

https://doi.org/10.1021/jacs.2c05096
J. Am. Chem. Soc. 2022, 144, 14446−14451

Scheme 1. Protonation of (BPI)Pt(CH_3) to Form [^{H}(BPI)Pt(CH_3)][OTf] Followed by Thermolysis to Form Methane and (BPI)Pt(OTf)

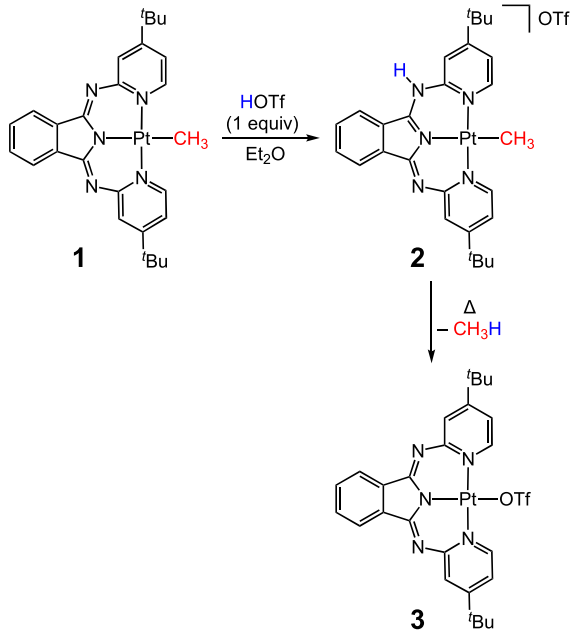

ligand and significant hydrogen bonding between $^-$OTf and the amine proton (N–O distance = 2.805(4) Å).[20]

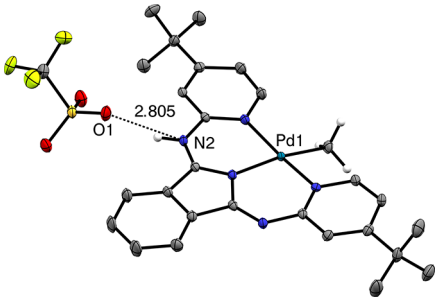

Figure 1. Solid-state structure of **2-Pd**. Thermal ellipsoids are shown at 50% probability, and hydrogens of the BPI ligand (except the N–H) are omitted for clarity.

Heating a red solution of the protonated species, **2**, in C_6D_6 at 60 °C (6 h) resulted in the formation of yellow (BPI)Pt(OTf) (**3**) and the liberation of methane[21] (Scheme 1), as observed by ^{1}H NMR spectroscopy. The crystal structure of **3** shows a metal-bound triflate (Figure S25), and the ^{19}F{^{1}H} NMR spectrum shows evidence of the triflate changing from a counterion in **2** (−78.0 ppm) to coordinated in **3** (−76.9 ppm).[22,23]

The kinetics of the C–H coupling reaction were monitored using UV–vis spectroscopy. Spectra of the reaction in toluene (Figure 2a) show four isosbestic points, indicating that there is no significant accumulation of intermediates in the reaction.

Data for the disappearance of **2** with respect to time fit an exponential decay (Figure 2b), confirming the rate is first-order in substrate, [^{H}(BPI)Pt(CH_3)][OTf]. An Eyring analysis (50–90 °C) yields a $\Delta H^{\ddagger}$ = 25.6 ± 0.5 kcal mol^{-1} and $\Delta S^{\ddagger}$ = 0.3 ± 1.5 cal/K·mol ($\Delta G^{\ddagger}$ = 25.5 ± 0.7 kcal mol^{-1} at 25 °C). A kinetic isotope effect (KIE) was determined (1.17 ± 0.05, 80

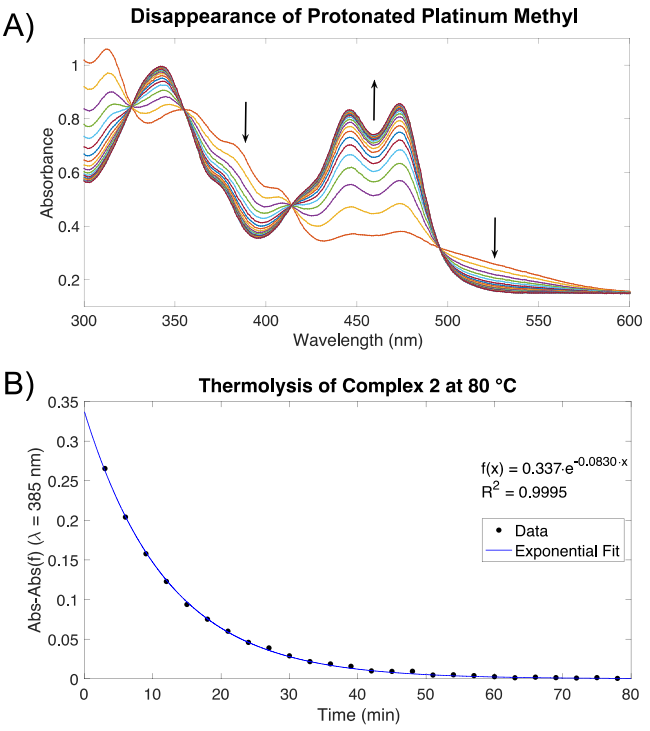

Figure 2. (A) UV–vis spectra of the disappearance of **2** over time at 80 °C. (B) First-order exponential fit of the data at 385 nm.

°C) via kinetic monitoring of the reaction of **2-d_1** in which the amine nitrogen was deuterated.

The first step of the C–H coupling reaction from **2** is proposed to be transfer of the amine proton either to the metal or directly to the methyl. As water or alcohol has been reported to act as a proton shuttle in some systems,[24,25] the thermolysis of **2** (50 μM) in toluene was repeated at 80 °C in the presence of methanol (625 μM). The similarity of the measured rate constant ((13.6 ± 0.2) × 10^{-4} s^{-1}) to that observed without added methanol ((13.8 ± 0.3) × 10^{-4} s^{-1}) argues against methanol assistance.

Density functional theory (DFT) was then employed to probe potential mechanisms for the C–H coupling reaction. To reduce computational cost, the *tert*-butyl groups were replaced by methyl groups. A direct proton transfer pathway from the amine to the Pt-methyl could not be found. The tautomerization of **2**, wherein the proton moves to the Pt center to form the Pt^{IV} intermediate [(BPI)Pt(CH_3)(H)]$^+$, was then considered. Initially, direct proton transfer from the amine to the Pt to form [(BPI)Pt(CH_3)(H)]$^+$ (**C**) without any anion interaction was analyzed (Figure 3). It is notable that dissociation of $^-$OTf from **2** to give cationic [^{H}(BPI)Pt-(CH_3)]$^+$ (**A**) is disfavored ($\Delta G°$ = 29.5 kcal mol^1). Direct transfer of the backbone proton to the Pt in this cation was found to be further endergonic (**C**, $\Delta G°$ = 55.1 kcal mol^{-1}), with a very high kinetic barrier (**B**, $\Delta G^{\ddagger}$ = 84.9 kcal mol^{-1}). Attempts to move the proton around the chelation ring of the ligand through interaction with the pyridine or indole nitrogens resulted in prohibitively high energy transition states (TSs).[20] These high-energy pathways led to consideration of whether the counteranion, triflate, could be acting as a proton shuttle and assisting in the formation of the C–H bond.

Deprotonation of [^{H}(BPI)Pt(CH_3)]$^+$ by triflate to form the separated neutral species (BPI)Pt(CH_3) (**1**) and HOTf is accessible ($\Delta G°$ = 19.4 kcal mol^{-1}) (Figure 4). A low-energy

https://doi.org/10.1021/jacs.2c05096
J. Am. Chem. Soc. 2022, 144, 14446–14451

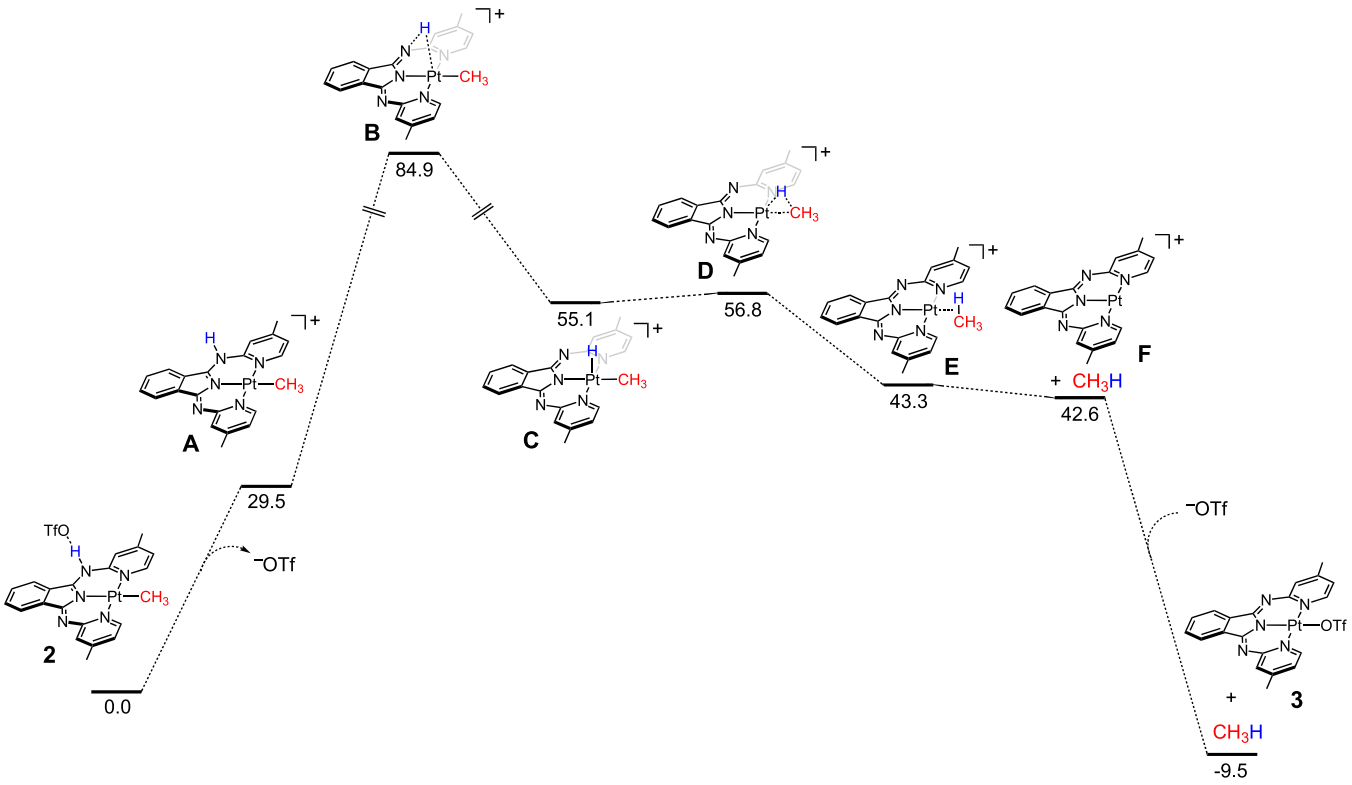

Figure 3. Calculated energies for the anion-free reaction of **2** to release methane with ΔG and $\Delta G^{\ddagger}$ reported in kcal mol^{-1}. PBE0-D3//6-311++G(d,p)/LANL2TZ with implicit toluene solvation (SMD).

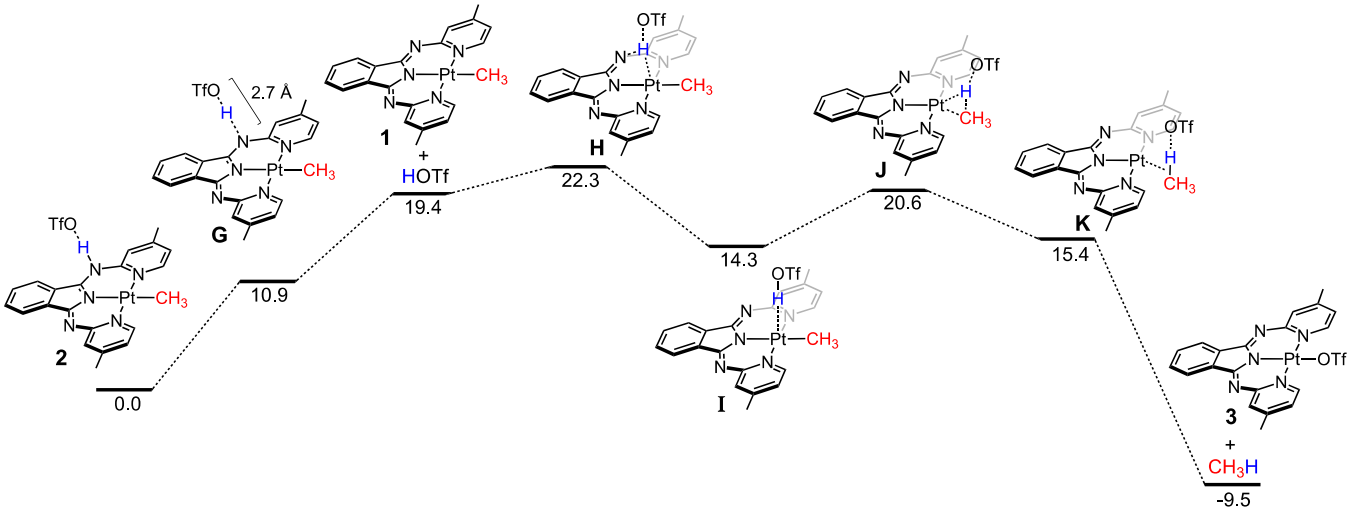

Figure 4. Calculated energies for the anion-assisted conversion of **2** to **3**. ΔG and $\Delta G^{\ddagger}$ are reported in kcal mol^{-1}. PBE0-D3//6-311++G(d,p)/LANL2TZ with implicit toluene solvation (SMD) was used.

transition state for transfer of the proton from the backbone N to the Pt interaction was located (**H**, $\Delta G^{\ddagger}$ = 22.3 kcal mol^{-1}), with HOTf located midway between the imine nitrogen and Pt. Intrinsic reaction coordinate and subsequent geometry optimization calculations from this TS confirmed that it proceeded to **2** on one side and a five-coordinate adduct, (BPI)Pt(CH_3)(HOTf) (**I**, ΔG° = 14.3 kcal mol^{-1}), on the other.

A relaxed angle scan of the Pt−N_{immine}−O(H) angle from this TS toward the starting material (Figure S21) showed a downhill potential energy surface with no additional barriers, suggesting that it is equally feasible to form **1** and HOTf or to maintain the (BPI)Pt(CH_3)/HOTf interaction prior to formation of the transition state. A crossover study to examine whether triflic acid completely dissociates from **2** during the thermolysis reaction was inconclusive.[26]

In comparison to $[(BPI)Pt^{IV}(CH_3)(H)]^+$ (**C**) considered above, the Pt−H distance in (**I**) is significantly elongated (Δ = 0.57 Å), and the H−OTf distance is only slightly different than that calculated for free HOTf (Δ = +0.06 Å, Figure S17). Based on this analysis, the intermediate is a Pt^{II} triflic acid adduct rather than a Pt^{IV} hydride (Figure S17). The subsequent C−H bond formation transition state (**J**) was located at $\Delta G^{\ddagger}$ = 20.6 kcal mol^{-1}, which proceeded to a

https://doi.org/10.1021/jacs.2c05096
J. Am. Chem. Soc. 2022, 144, 14446−14451

methane σ-complex (**K**, $\Delta G^{\ddagger}$ = 15.4 kcal mol^{-1}). The release of methane and binding of $^{-}$OTf to Pt is significantly favored and overall conversion of **2** to **3** and methane is downhill by ΔG° = −9.5 kcal mol^{-1}. Notable is that formation of a Pt^{IV} intermediate is avoided in this MLAC C−H bond formation mechanism.

The highest calculated barrier, **H** (Figure 4, ΔG° = 22.3 kcal mol^{-1}), was also investigated with the full *tert*-butyl-substituted rather than methyl-substituted BPI ligand, and a very similar barrier ($\Delta G^{\ddagger}$ = 22.5 kcal mol^{-1}) was determined. Furthermore, the DFT-calculated KIE for this step was 1.19, in agreement with the experimental KIE of 1.17 ± 0.05. In contrast, if the transition state for C−H bond formation, **J** (Figure 4, ΔG° = 20.6 kcal mol^{-1}), were rate determining, DFT predicts a KIE of 1.59.

If the triflic acid completely dissociates from **2**, an interaction of HOTf with a second Pt in the form of **2** is also possible, yielding [^{H}(BPI)Pt(CH$_3$)(HOTf)][OTf] (ΔG° = 15.2 kcal mol^{-1}, Figure S14). However, a higher barrier was computed to form the Pt−CH$_4$ adduct from this species ($\Delta G^{\ddagger}$ = 26.1 kcal mol^{-1}) relative to that from **I**. In addition, such a mechanism would give rise to second-order kinetic dependence on [**2**], inconsistent with the experimental data.

The role of the anion was further explored by the addition of HCl to **1** or (*n*-Bu)$_4$Cl to **2**; both experiments resulted in rapid formation of (BPI)PtCl (**4**) and methane at room temperature. When (*n*-Bu)$_4$Cl was added to **2** at −63 °C, ^{1}H NMR signals for a new species with one N−H peak (14.70 ppm) and broken symmetry of the ligand were observed. These signals disappeared above −10 °C to form **4**, suggesting that [^{H}(BPI)Pt(CH$_3$)][Cl] had formed and underscoring the dramatic effect of the anion on the C−H coupling reaction. DFT studies with $^{-}$Cl instead of $^{-}$OTf show significantly decreased energies for all intermediates and TSs.[20]

There are only a few studies where Pt complexes with a proton stored on the ligand and a methyl bound to the metal were thermolyzed to form methane.[27−30] Puddephatt reported a Pt^{II}-methyl complex where the kinetic site of protonation was a pendant amine arm.[27] Subsequent formation of a Pt^{IV}−H intermediate followed by C−H reductive elimination was proposed. Nozaki found that a cationic hydroxycyclopentadienyl methylplatinum^{IV} species underwent reductive elimination of methane with formation of a Pt^{II} product.[28] The transformation from Pt^{IV} to Pt^{II} was proposed to involve an MLC mechanism with a trifluoroacetate anion assisting in the transfer of the proton from the hydroxycyclopentadienyl to the methyl.

The propensity of the microscopic reverse reaction, a C−H bond activation by a MLC-like mechanism, was examined within the (BPI)Pt system. No benzene activation product was observed, even after heating (BPI)Pt(OTf) (**3**) in C$_6$D$_6$ to 200 °C. In contrast, MLC bond activations were observed for H$_2$ and phenylacetylene substrates. Heating a C$_6$D$_6$ solution of **3** under H$_2$ (5 atm) for 20 h at 100 °C resulted in formation of [^{H}(BPI)Pt(H)][OTf] (**5**), and C−H activation of phenylacetylene in C$_6$D$_6$ was observed at room temperature, producing [^{H}(BPI)Pt(CCPh)][OTf] (**6**) within two hours. Given that the C−H bond of benzene is more similar to that of methane than of phenylacetylene, the lack of C−H activation of benzene by **3** could be explained by the triflate being too strongly bound to allow benzene to enter the coordination sphere of the platinum and react. The coordination of $^{-}$OTf to the (BPI)Pt open-site compound is very favorable (ΔG° = −53 kcal/mol), but the coordination of the more weakly binding, less basic triflimide counterion is less favorable (ΔG° = −47 kcal/mol). Indeed, a compound analogous to **2** but with a triflimide counterion, [^{H}(BPI)Pt(CH$_3$)][NTf$_2$] (**7**), showed activity for arene C−H bond activation after methane elimination. In C$_6$D$_6$, the N−H shift in the ^{1}H NMR spectrum for **7** is at 10.78 ppm vs 13.10 ppm for **2**, suggesting a substantially weaker interaction of the triflimide with the proton on the ligand backbone. Thermolysis of **7** in C$_6$H$_6$ at 100 °C for 15 h resulted in the release of methane and formation of a new metal species in 30% yield as the major product by ^{1}H NMR spectroscopy (Scheme 2).[20] Comparison

Scheme 2. Activation of Benzene by 7

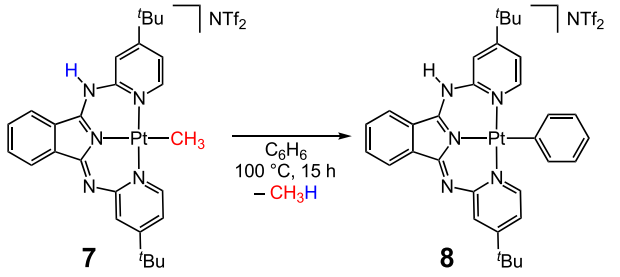

to an authentic sample of [^{H}(BPI)Pt(C$_6$H$_5$)][NTf$_2$] (**8**) confirmed the formation of the phenyl complex. If the reaction was carried out in C$_6$D$_6$, CH$_4$ was the only methane isotopologue formed. Thus, informed by the mechanistic studies of the triflate system, use of a weaker-coordinating anion allowed for the activation of benzene C−H bonds across the Pt and ligand backbone.

The studies reported herein add new understanding to the activation of C−H bonds using MLC. The anion assists in the proton transfer between the metal and the ligand, and in doing so, a high oxidation state Pt^{IV} intermediate is avoided. Thus, the basicity of the anion and conversely the acidity of the metal active site comprise critical design features in promoting the selective activation of strong, nonpolar C−H bonds via MLAC mechanisms.

■ ASSOCIATED CONTENT

Supporting Information

The Supporting Information is available free of charge at https://pubs.acs.org/doi/10.1021/jacs.2c05096.

Synthetic and experimental procedures, characterization of new compounds, kinetic data and analysis, and computational methods (PDF)

Accession Codes

CCDC 2129748−2129750 contain the supplementary crystallographic data for this paper. These data can be obtained free of charge via www.ccdc.cam.ac.uk/data_request/cif, or by emailing data_request@ccdc.cam.ac.uk, or by contacting The Cambridge Crystallographic Data Centre, 12 Union Road, Cambridge CB2 1EZ, UK; fax: +44 1223 336033.

■ AUTHOR INFORMATION

Corresponding Author

Karen I. Goldberg − *Department of Chemistry, University of Pennsylvania, Philadelphia, Pennsylvania 19104, United States;* orcid.org/0000-0002-0124-1709; Email: kig@sas.upenn.edu

https://doi.org/10.1021/jacs.2c05096
J. Am. Chem. Soc. 2022, 144, 14446−14451

Authors

Hannah E. Zeitler − *Department of Chemistry, University of Pennsylvania, Philadelphia, Pennsylvania 19104, United States*

Alexander S. Phearman − *Department of Chemistry, University of Pennsylvania, Philadelphia, Pennsylvania 19104, United States;* orcid.org/0000-0003-3858-1261

Michael R. Gau − *Department of Chemistry, University of Pennsylvania, Philadelphia, Pennsylvania 19104, United States;* orcid.org/0000-0002-4790-6980

Patrick J. Carroll − *Department of Chemistry, University of Pennsylvania, Philadelphia, Pennsylvania 19104, United States*

Thomas R. Cundari − *Department of Chemistry and Center for Advanced Scientific Computing and Modeling, University of North Texas, Denton, Texas 76203, United States;* orcid.org/0000-0003-1822-6473

Complete contact information is available at: https://pubs.acs.org/10.1021/jacs.2c05096

Notes

The authors declare no competing financial interest.

■ ACKNOWLEDGMENTS

This work was supported by the National Science Foundation (CHE-1856547). This work used the Extreme Science and Engineering Discovery Environment (XSEDE)[31] Expanse cluster (TG-CHE190112) at the San Diego Supercomputer Center, which is supported by the National Science Foundation (ACI-1548562). T.R.C. acknowledges the NSF (CHE-1953547) for partial support of this research.

■ REFERENCES

(1) Goldberg, K. I.; Goldman, A. S. Large-Scale Selective Functionalization of Alkanes. *Acc. Chem. Res.* **2017**, *50* (3), 620−626.

(2) Gunsalus, N. J.; Koppaka, A.; Park, S. H.; Bischof, S. M.; Hashiguchi, B. G.; Periana, R. A. Homogeneous Functionalization of Methane. *Chem. Rev.* **2017**, *117* (13), 8521−8573.

(3) Labinger, J. A. Platinum-Catalyzed C−H Functionalization. *Chem. Rev.* **2017**, *117* (13), 8483−8496.

(4) Lapointe, D.; Fagnou, K. Overview of the Mechanistic Work on the Concerted Metallation−Deprotonation Pathway. *Chem. Lett.* **2010**, *39* (11), 1118−1126.

(5) Yang, L.; Zhang, Q.; Gao, J.; Wang, Y. Why Can Normal Palladium Catalysts Efficiently Mediate Aerobic C−H Hydroxylation of Arylpyridines by Intercepting Aldehyde Autoxidation? A Nascent Palladium(III)−Peracid Intermediate Makes a Difference. *Inorg. Chem.* **2019**, *58* (7), 4376−4384.

(6) Engle, K. M.; Wang, D.-H.; Yu, J.-Q. Ligand-Accelerated C−H Activation Reactions: Evidence for a Switch of Mechanism. *J. Am. Chem. Soc.* **2010**, *132* (40), 14137−14151.

(7) Jia, X.; Frye, L. I.; Zhu, W.; Gu, S.; Gunnoe, T. B. Synthesis of Stilbenes by Rhodium-Catalyzed Aerobic Alkenylation of Arenes via C−H Activation. *J. Am. Chem. Soc.* **2020**, *142* (23), 10534−10543.

(8) Rubashkin, S. B.; Chu, W.-Y.; Goldberg, K. I. Lowering the Barrier to C−H Activation at Ir^{III} through Pincer Ligand Design. *Organometallics* **2021**, *40* (9), 1296−1302.

(9) Higashi, T.; Kusumoto, S.; Nozaki, K. Cleavage of Si−H, B−H, and C−H Bonds by Metal−Ligand Cooperation. *Chem. Rev.* **2019**, *119* (18), 10393−10402.

(10) Khusnutdinova, J. R.; Milstein, D. Metal−Ligand Cooperation. *Angew. Chem., Int. Ed.* **2015**, *54* (42), 12236−12273.

(11) Leeb, N. M.; Drover, M. W.; Love, J. A.; Schafer, L. L.; Slattery, J. M. Phosphoramidate-Assisted Alkyne Activation: Probing the Mechanism of Proton Shuttling in a N,O-Chelated Cp*Ir(III) Complex. *Organometallics* **2018**, *37* (24), 4630−4638.

(12) Galiana-Cameo, M.; Urriolabeitia, A.; Barrenas, E.; Passarelli, V.; Pérez-Torrente, J. J.; Di Giuseppe, A.; Polo, V.; Castarlenas, R. Metal−Ligand Cooperative Proton Transfer as an Efficient Trigger for Rhodium-NHC-Pyridonato Catalyzed gem-Specific Alkyne Dimerization. *ACS Catal.* **2021**, *11* (12), 7553−7567.

(13) Noyori, R.; Hashiguchi, S. Asymmetric Transfer Hydrogenation Catalyzed by Chiral Ruthenium Complexes. *Acc. Chem. Res.* **1997**, *30* (2), 97−102.

(14) Schwartsburd, L.; Iron, M. A.; Konstantinovski, L.; Diskin-Posner, Y.; Leitus, G.; Shimon, L. J. W.; Milstein, D. Synthesis and Reactivity of an Iridium(I) Acetonyl PNP Complex. Experimental and Computational Study of Metal−Ligand Cooperation in H−H and C−H Bond Activation via Reversible Ligand Dearomatization. *Organometallics* **2010**, *29* (17), 3817−3827.

(15) Ben-Ari, E.; Leitus, G.; Shimon, L. J. W.; Milstein, D. Metal−Ligand Cooperation in C−H and H_2 Activation by an Electron-Rich PNP Ir(I) System: Facile Ligand Dearomatization−Aromatization as Key Steps. *J. Am. Chem. Soc.* **2006**, *128* (48), 15390−15391.

(16) Higashi, T.; Kusumoto, S.; Nozaki, K. Heterolytic Oxidative Addition of sp^2 and sp^3 C−H Bonds by Metal−Ligand Cooperation with an Electron-Deficient Cyclopentadienone Iridium Complex. *J. Am. Chem. Soc.* **2021**, *143* (33), 12999−13004.

(17) Schwartsburd, L.; Iron, M. A.; Konstantinovski, L.; Ben-Ari, E.; Milstein, D. A Dearomatized Anionic PNP Pincer Rhodium Complex: C−H and H−H Bond Activation by Metal−Ligand Cooperation and Inhibition by Dinitrogen. *Organometallics* **2011**, *30* (10), 2721−2729.

(18) Zeitler, H. E.; Kaminsky, W. A.; Goldberg, K. I. Insertion of Molecular Oxygen into the Metal−Methyl Bonds of Platinum(II) and Palladium(II) 1,3-Bis(2-pyridylimino)isoindolate Complexes. *Organometallics* **2018**, *37*, 3644−3648.

(19) Ho, S. K. Y.; Lam, F. Y. T.; de Aguirre, A.; Maseras, F.; White, A. J. P.; Britovsek, G. J. P. Photolytic Activation of Late-Transition-Metal−Carbon Bonds and Their Reactivity toward Oxygen. *Organometallics* **2021**, *40* (24), 4077−4091.

(20) See the Supporting Information for more details.

(21) By comparison with an internal standard, 42% of the expected total amount of methane was observed in solution by ^{1}H NMR spectroscopy. Methane in the headspace of the sample was not accounted for.

(22) Burns, R. M.; Hubbard, J. L. Alkyne Activation by Electrophilic $[(\eta\text{-}C_5Me_5)Ru(NO)(R)]^+$ (R = Me, Ph, *p*-tolyl) Fragments: *β*-Migratory Insertion, Isomerization, and Metallacycle Formatio. *J. Am. Chem. Soc.* **1994**, *116* (21), 9514−9520.

(23) Hayashida, T.; Kondo, H.; Terasawa, J.-i.; Kirchner, K.; Sunada, Y.; Nagashima, H. Trifluoromethanesulfonate (triflate) as a moderately coordinating anion: Studies from chemistry of the cationic coordinatively unsaturated mono- and diruthenium amidinates. *J. Organomet. Chem.* **2007**, *692* (1), 382−394.

(24) Smith, N. E.; Bernskoetter, W. H.; Hazari, N. The Role of Proton Shuttles in the Reversible Activation of Hydrogen via Metal−Ligand Cooperation. *J. Am. Chem. Soc.* **2019**, *141* (43), 17350−17360.

(25) Bielinski, E. A.; Förster, M.; Zhang, Y.; Bernskoetter, W. H.; Hazari, N.; Holthausen, M. C. Base-Free Methanol Dehydrogenation Using a Pincer-Supported Iron Compound and Lewis Acid Co-catalyst. *ACS Catal.* **2015**, *5* (4), 2404−2415.

(26) $[^H(BPI)Pt(CH_3)][OTf]$ (**2**) and $[^D(BPI)Pt(CD_3)][OTf]$ (**2-*d*$_4$**) were heated together in toluene-d_8 at 80 °C. The formation of **3**, as well as CH_4, CH_3D, and CD_3H, was observed by ^{1}H NMR spectroscopy. While this result is consistent with free HOTf and DOTf, exchange of the N−H(D) in the starting material prior to methane elimination could not be ruled out; attempts to determine if such scrambling was occurring before the reaction were inconclusive.

(27) Higashi, T.; Ando, H.; Kusumoto, S.; Nozaki, K. Metal−Ligand Cooperative C−H Bond Formation by Cyclopentadienone Platinum Complexes. *J. Am. Chem. Soc.* **2019**, *141* (6), 2247−2250.

(28) Hinman, J. G.; Baar, C. R.; Jennings, M. C.; Puddephatt, R. J. Protonolysis of Dimethylplatinum(II) Complexes: Primary Attack at Metal or Ligand. *Organometallics* **2000**, *19* (4), 563−570.
(29) Vedernikov, A. N.; Pink, M.; Caulton, K. G. Hydrocarbyl Ligand "Tuning" of the $Pt^{II/IV}$ Redox Potential. *Inorg. Chem.* **2004**, *43* (12), 3642−3646.
(30) Britovsek, G. J. P.; Taylor, R. A.; Sunley, G. J.; Law, D. J.; White, A. J. P. Protonation of Platinum(II) Dialkyl Complexes Containing Ligands with Proximate H-Bonding Substituents. *Organometallics* **2006**, *25* (8), 2074−2079.
(31) Towns, J.; Cockerill, T.; Dahan, M.; Foster, I.; Gaither, K.; Grimshaw, A.; Hazlewood, V.; Lathrop, S.; Lifka, D.; Peterson, G. D.; Roskies, R.; Scott, J.; Wilkins-Diehr, N. *XSEDE: Accelerating Scientific Discovery*. **2014**, *16* (05), 74.

NOTE ADDED AFTER ASAP PUBLICATION

This paper was published on July 26, 2022. Chart 1 has been updated and the revised version was re-posted on August 3, 2022.

https://doi.org/10.1021/jacs.2c05096
J. Am. Chem. Soc. 2022, 144, 14446−14451